



Corrosion behaviour of Aluminium 6061/ Red mud metal matrix composites in alkaline medium

P.V. Krupakara¹, C. Anbuselvan², S. Balasubramanian², E.K. Manoharan² and M. Singanan^{2*}

¹ Department of Chemistry, Cambridge Institute of Technology, North Campus, Lingadheera Golla Halli, Kundana Post, Devanahalli Taluk, Bangalore – 562110, Karnataka, India.

² Department of Chemistry, Presidency College (Autonomous), Chennai – 600005, Tamil Nadu, India.

*Corresponding Author

Email: swethasinganan1966@gmail.com

Abstract

In recent years, the research and developments in the field of application of aluminium metal matrix composites are increasing due to wider industrial needs. This is due to the improvements in density, mechanical and corrosion behaviour of aluminium-based alloys. In this research paper corrosion behaviour of aluminium 6061 / red mud metal matrix composites is discussed with respect to microstructure, static weight loss corrosion and potentiodynamic polarization. Composites containing three different percentages of red mud particulates are manufactured by liquid melt metallurgy technique using vortex method. Matrix alloy and composites are tested for corrosion behaviour in three different concentrated solutions of sodium hydroxide. Results obtained reveal that in all the tests the corrosion rate of composite materials decrease with increase in reinforcement content when compared to matrix alloy in alkaline medium. Hence composites are more suitable for application in alkaline medium.

Keywords: Aluminium, red mud, static weight loss, polarization, vortex

Introduction

The aluminium 6061 alloy or amalgam is one of the massively used in industrial applications due to its considerable mechanical and corrosion behaviour. The fabrication of metal matrix composites using aluminium 6061 as metal frame work (matrix) and addition of reinforcements or fortifications like many ceramic particulates have caused improved mechanical strength, corrosion behaviour. The usage of this composite materials is found in almost all the fields of industries and engineering especially in automobile, marine and aerospace. The composites possess diminished weight high strength. They are replacing heavy metals like cast iron and bronze which were popular in the past¹. As increased number of materials are required with extended strength and diminished weight, there is a big possibility of growth of such materials. Many researchers have studied mechanical behaviour and corrosion behaviour of aluminium-based alloys reinforced with various ceramic particulates like quartz, titanium dioxide, red mud, basalt fiber, beryl, glass fibers, albite, silicon carbide and garnet²⁻¹². Extensive literature survey reveals that studies with respect to corrosion behaviour of aluminium 6061 reinforced with red mud particulates in alkaline medium like sodium hydroxide solution has not been studied so far. Hence this work has been taken up.

Experimental procedure

Material selection

Raw material selected is aluminium 6061 framework amalgam (matrix alloy) which is available commercially. The purchased alloy was tested for the composition and it presented in the Table 1 given below.

Table 1. Composition (in %) of Al 6061 Alloy.

Mg	Si	Fe	Cu	Ti	Pb	Zn	Mn	Sn	Ni	Al
0.8-1.5	10-12	1.0	0.7-1.5	0.2	0.1	0.5	0.5	0.1	1.5	Bal

Due to the higher concentration of magnesium and silicon in the alloy the number is given as 6061 as per ASTM norms. Figure 1 below shows the commercially procured aluminium 6061 alloy. The reinforcement or fortification used in this work for the manufacture of composite materials is red mud. It is a waste material obtained during the extraction of aluminium from its ore bauxite. Figure 2 below shows the red mud. It is procured from HINDALCO, Renukoot District, UP, India.



Figure1. Aluminium 6061 alloy.



Figure 2. Red mud particulates.

Energy dispersive x-ray spectroscopy studies (EDAX) of red mud reveals that it mainly contains silica and oxides of iron, titanium, zirconium and vanadium. EDAX spectrum is given below in Figure 3.

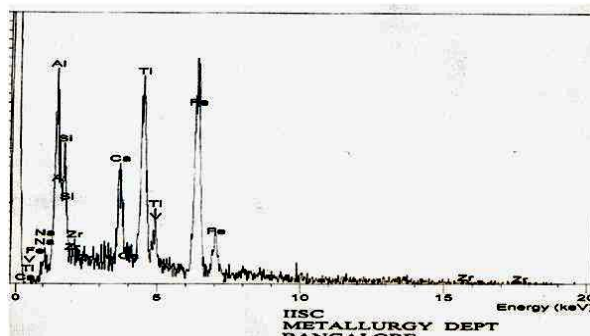


Figure 3. EDAX studies of red mud.

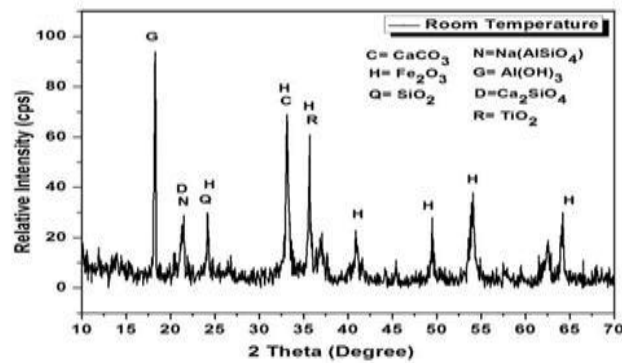


Figure 4. XRD analysis of red mud.

The main components found in the XRD analysis given in Figure 4 above are hematite (Fe_2O_3), Gibbsite ($\text{Al}(\text{OH})_3$), Rutile (TiO_2), Calcite (CaCO_3), sodium aluminium silicate (NaAlSiO_4), Calcium silicate (Ca_2SiO_4) and quartz (SiO_2). The experiments are conducted in the different concentrated solutions of research grade sodium hydroxide.

Composite preparation

Composites are prepared using above mentioned raw materials by liquid melt metallurgy technique using vortex method. It is also named as stir casting method. The furnace used for the preparation of the aluminium-red mud particulate composite basically contains an electrically heated 3 phase resistance coil thus the furnace is fitted with three pairs of 14-gauge kanthal, which are A₁ grade heating coils. The temperature range of the furnace is 1200°C with a temp control accuracy of $\pm 1^\circ\text{C}$. The furnace is fitted with a graphite crucible at its center with opening provision at bottom, which enables to pour the melt directly into mould which is as shown in Figure 5 below. Red mud particulate size was selected was $50\text{-}80\ \mu\text{m}$ based on the experience and reference to various technical reports. The weight of percentage of red mud particulates selected was 2-6% insteps of 2%. Aluminium 6061 matrix is heated above 600°C , melt was degassed using nitrogen gas. Mechanical stirrer coated with aluminite (to prevent migration of ferrous ions from the stirrer material into the aluminium 6061 melt) is used to create the vortex. It is rotated at a speed of 400 rpm. Uncoated red mud particulates which are pre heated in a muffle furnace at 400°C is added to the melt at a rate of 120 g/min. Hexachloroethane tablets shown in Figure 6 below is added to the melt to remove entrapped air and gas bubbles. The molten mixture was then poured into pre heated cast iron moulds directly from the bottom of the furnace. Castings were produced in the form of cylindrical rods of diameter 30 mm and length 150 mm.



Figure 5. Bottom pouring furnace.



Figure 6. Hexachloroethane tablet.

Aluminium 6061 amalgam containing 2,4 and 6 weight percentage of red mud particulates are casted as per above procedure mentioned. Aluminium 6061 alloy without any fortifications is also casted in the same manner to compare the results. Krupakara¹³ adopted same method for the preparation of composites.

Specimen preparation

The castings of composites and metal amalgam were subjected to machining in CNC lathe machine to get cylindrical specimen of 20 mm diameter and 20 mm length. The samples were successively ground using 240, 320, 400, and 600 SiC paper and were polished according to standard metallographic techniques and dipped in acetone and dried. The samples were weighed up to fourth decimal place using electronic balance and also the specimen dimensions were noted down using slide callipers. These specimens were used for conducting static weight loss corrosion test. For conducting potentiodynamic polarization test rectangular specimen of dimension 2 cm length, 1 cm breadth and 1 mm thickness were machined from composites and amalgam.

Microstructural studies

Before the corrosion test the specimen of matrix and composites were subjected to microstructural studies using scanning electron microscopy. Figures 7-10, shows the microstructure of aluminium 6061 amalgam and its composites with fortifications of red mud particulates.

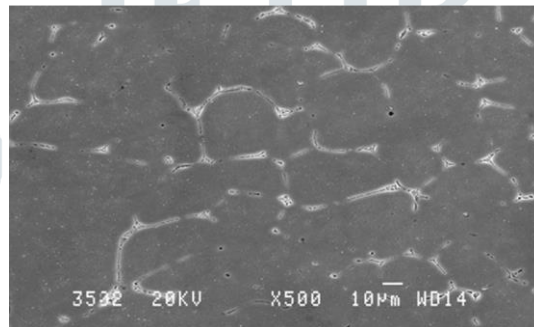


Figure 7. Microstructure of Al 6061 amalgam.

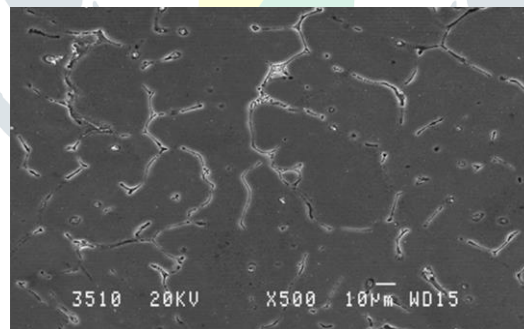


Figure 8. Microstructure of 2% composite.

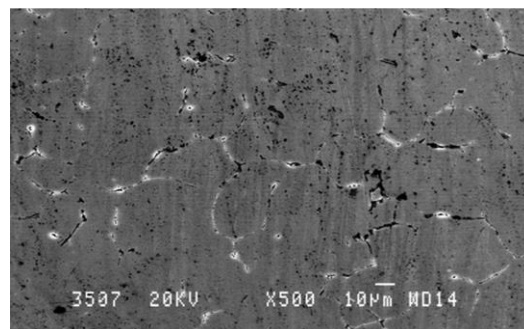


Figure 9. Microstructure of 4% composite.

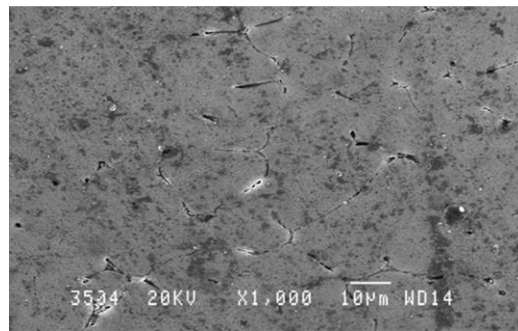


Figure 10. Microstructure of 6% composite.

Experimental procedure

The corrosion behaviour of aluminium/red mud composite materials with respect to static weight loss corrosion test was studied by immersion method. By this method it is easy to measure the corrosion loss. The tests were conducted in 0.25N, 0.5N, and 1N solutions of sodium chloride. 200 ml of the prepared corrosive solutions were taken in series of beaker. Samples were suspended in the corrosive medium for different time intervals up to 96 h in the steps of 24 h. To minimize the contamination of the aqueous solution and loss due to evaporation, the beakers were covered with paraffin paper during the entire test period. After the specified time, the samples were cleaned mechanically using a brush to remove the heavy corrosion deposits on the surface. The corresponding changes in the weights were noted. Corrosion rates were computed using the equation. Corrosion rate = $534 W/DAT$ mpy. Where W is the weight loss in g, D is density of the specimen in g/cc, A is the area of the specimen (inch²) and T is the exposure time in hours¹⁴.

For potentiodynamic polarization test electrochemical work station CHI 608E series model developed by CH instruments USA. It has arrangement for a cell with reference electrode like calomel electrode, counter electrode like platinum electrode and also prepared specimen as working electrode. Polarization tests are also conducted in different concentrated solutions of sodium chloride.

Results and discussion

Figures 11, 12 and 13 are the graphical representation of results of static weight loss corrosion test in three different concentrated solutions of sodium hydroxide.

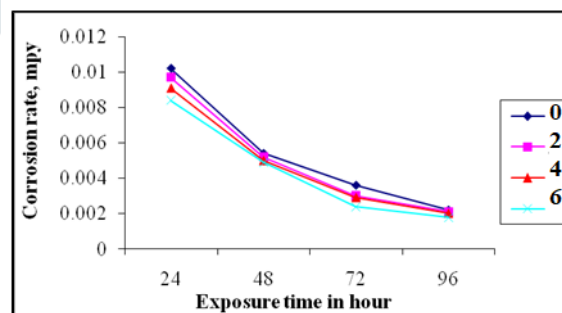


Figure 11. Weight loss corrosion in 0.25N NaOH.

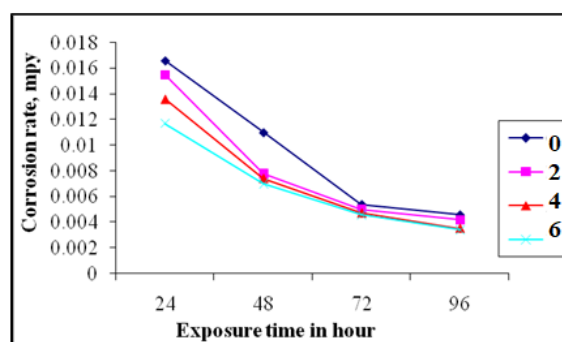


Figure 12. Weight loss corrosion in 0.5N NaOH.

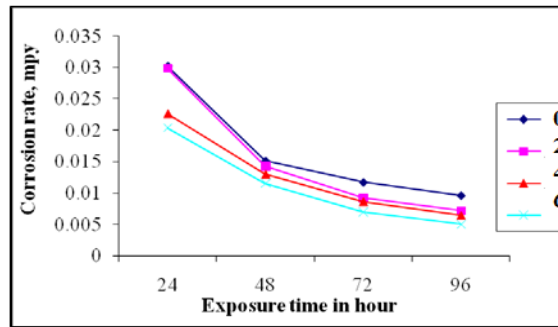


Figure 13. Weight loss corrosion in 1 N NaOH.

The above graphs are drawn by taking corrosion rates of amalgam and composites calculated using the formula given above on Y axis and time of exposure on X axis. Each graph shows four different coloured lines for alloy or amalgam (0) and for composites containing 2,4 and 6 weight percentage of red mud in the same amalgam. Microstructures of aluminium 6061 amalgam and composite materials were taken after corrosion test in 1N NaOH exposed for 96 hours are given below in Figures 14 – 17 respectively.

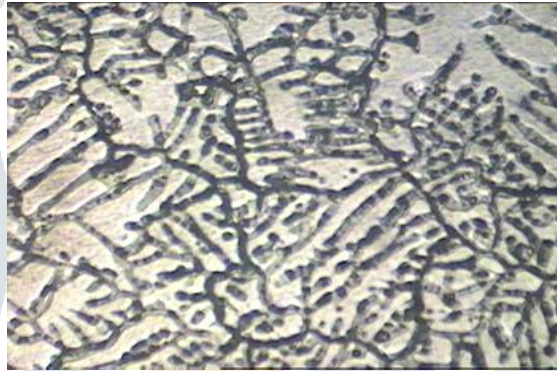


Figure 14. Microstructure of Al 6061 amalgam.

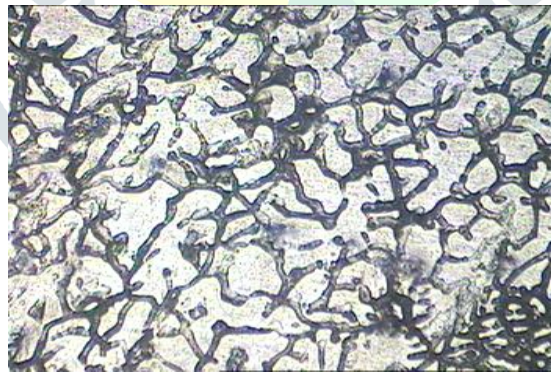


Figure 15. Microstructure of 2% composite.

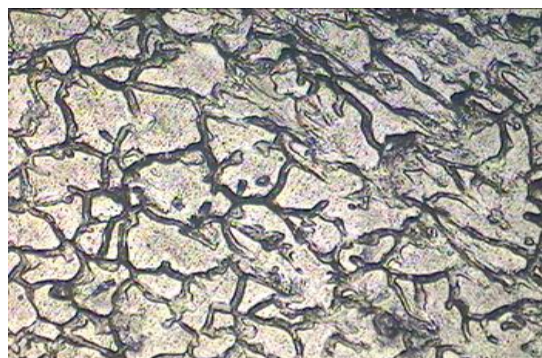


Figure 16. Microstructure of 4% composite.

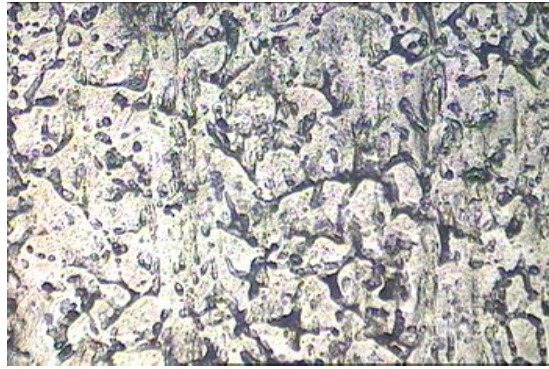


Figure 17. Microstructure of 6% composite.

The above microstructures are taken after removal of corrosion product in the form of deposit and flakes. Then washed thoroughly in distilled water and acetone. From the above microstructures it is clearly visible that matrix or amalgam of aluminium undergoes severe corrosion due to formation cracks. Extent of corrosion in the form of cracks goes on decreasing from 2% red mud particulate fortified composite to 6% red mud particulate fortified composite. Hence the corrosion rate decreases with increase in fortification content. Same type of results was obtained by other researchers for static weight loss corrosion test¹⁵⁻¹⁶. Figures 18 - 20 are the results of potentiodynamic polarization studies of aluminium 6061 amalgam and its composites containing red mud particulates in three different concentrated solutions of sodium hydroxide.

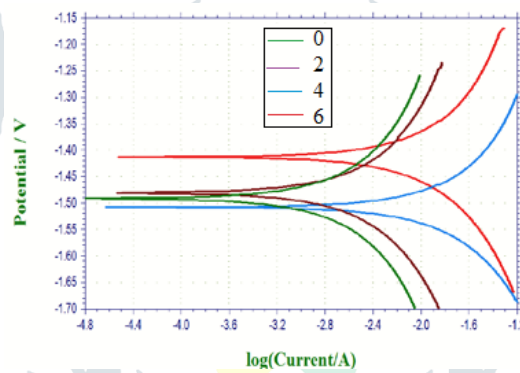


Figure 18. Polarization studies in 0.25N NaOH.

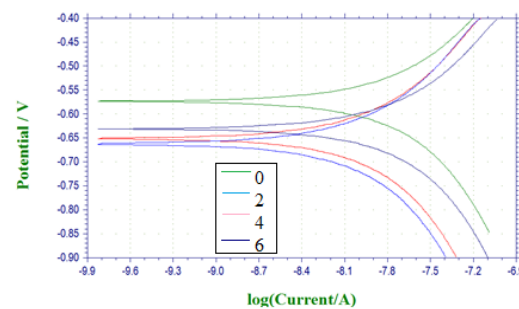


Figure 19. Polarization studies in 0.5N NaOH.

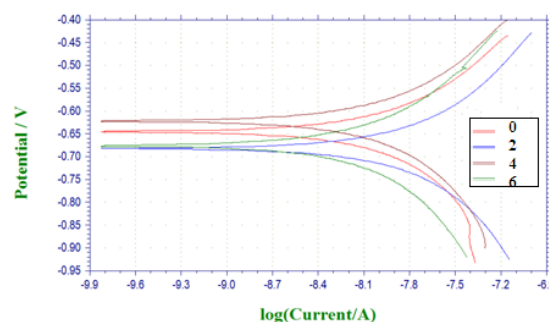


Figure 20. Polarization studies in 1N NaOH.

The graphs are drawn using the software and PC attached to the electrochemical workstation where the software calculates the corrosion rate directly and displays the same. In each graph four coloured curves are there for aluminium 6061 amalgam (0) and 2, 4 6 percent red mud reinforced composite materials. The corrosion rates in mpy (mills per year) shown by the electrochemical workstation are given in the Table 2 below.

Table 2. Corrosion rates in mpy in sodium nitrate solutions.

Percentage of Red mud	0	2	4	6
Concentration of NaOH	Corrosion rate in mpy			
0.25N	3.678	2.083	1.354	0.675
0.5N	3.681	2.845	1.3010	0.889
1N	4.207	3.304	2.388	1.755

The concentration of sodium hydroxide influences the corrosion rates of aluminium 6061 framework amalgam and its composites. As the concentration of sodium hydroxide increases the erosion rates also increases. The evolution of hydrogen gas increases with increase in concentration. The corrosion current and hydrogen gas liberation are directly proportional to each other and therefore rate of corrosion increases. Here the surface exposed to surrounding media will play an important role for the enhanced corrosion rates. The results depict that the rate of corrosion of aluminium 6061 framework amalgam and its composites decrease with increase in red mud content. Hence resistance to corrosion of composites is higher than framework amalgam. This can be attributed to the chemical inertness of fortification particulates which are ceramic in nature. The active surface area of metal framework exposed to the erosive media reduces due to the presence of fortification particulates, hence rate of erosion decreases. The microstructures of the aluminium 6061 amalgam and its composites taken after polarization test in 1N sodium hydroxide solution is given below in Figures 21 – 24.

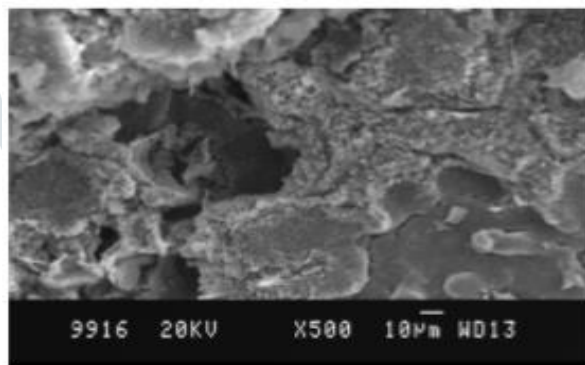


Figure 21. Microstructure of Al 6061 amalgam.

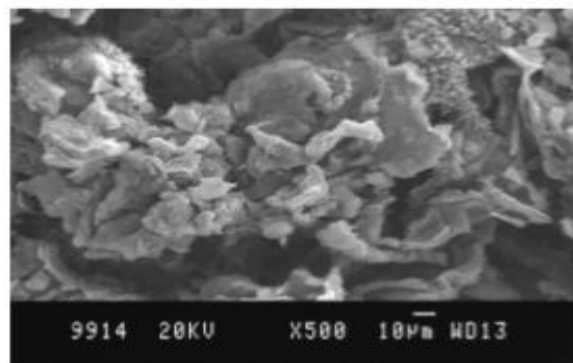


Figure 22. Microstructure of 2% composite.

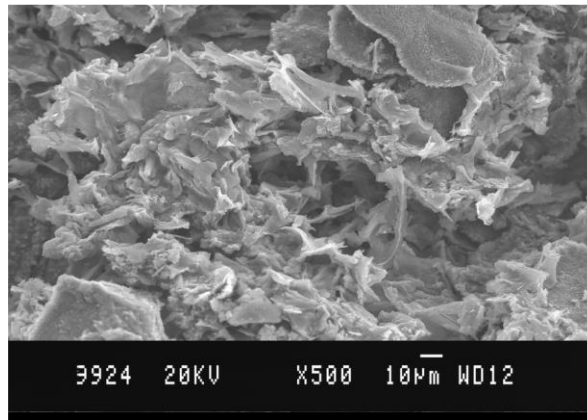


Figure 23. Microstructure of 4% composite.

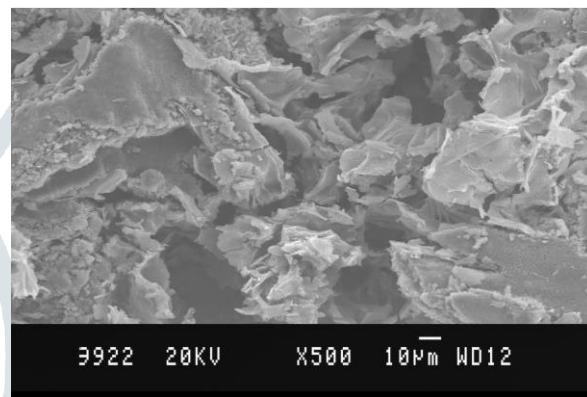


Figure 24. Microstructure of 6% composite.

In these microstructures also the metal framework exhibits a higher deep pits, cracks and flakes. But in the composites they are reducing with increase in the presence of red mud particulates fortification. Hence it can be clearly said that the composites exhibit higher corrosion resistance when compared to matrix amalgam due to the presence of inert, ceramic fortifications like red mud particulates. Several researchers have reported same type of results for their work on potentiodynamic polarization studies with different alloys of aluminium and fortifications¹⁷⁻¹⁹.

Conclusion

Composite materials made up of aluminium 6061 as matrix and red mud particulates as fortification were fabricated by stir casting method. Both matrix alloy and composites were subjected to static weight loss corrosion test and potentiodynamic polarization test in three different concentrated solutions of sodium hydroxide. Microstructures were also taken before and after the tests. In both tests the composite materials exhibited diminished corrosion rate when compared to aluminium 606 matrix or amalgam. Hence composite materials are more suitable than matrix alloy in many applications where alkaline atmosphere is created.

Bibliography

1. Jims John Wessley G, Srinivas S & Azgar Ali MD, International Journal of Engineering and Advanced Technology, 8(3S): 2019, 113-116.
2. Radha HR, Somashekariah BV, Krupakara PV & Vinutha K, International Journal of Chemical Sciences, 7(3): 2011, 503-507.
3. Vinutha K, Somashekariah BV, Krupakara PV & Radha HR, International Journal of Chemical Sciences, 6(1): 2010, 53-60.
4. Chandrashekar KN, Narasimha Murthy B & Krupakara. PV, International Journal of Engineering Science and Computing, 7(5): 2017, 11826-11830.

5. Elilvannan S & Paul Vizhian Simson, Journal of Chemical Engineering and Chemical Research, 1(2): 2014, 122-131.
6. Jayaprakash HV, Sachin Govind N & Krupakara PV, International Journal of Institutional and Industrial research, 3(1): 2018, 43-46.
7. Krishnaveni K, Radha HR & Krupakara PV, International Journal of Science Technology & Engineering, 6(4): 2019, 13-16.
8. Jayaprakash HV, International Journal of Basic and Applied Research, 8(12): 2018, 264-269.
9. Tejaswini A, Anusha MM & Krupakara PV. Stud Indian Place Names, 40(70): 2020, 3058-3062.
10. Ravishankar & Krupakara PV, Journal of Emerging Technologies and Innovative Research, 8(5), 2021, c48-c55.
11. Pruthviraj RD & Krupakara PV, Indian Journal of Chemistry and Environment, 10(3): 2007, 71-5.
12. Pruthviraj RD, Joseph V & Krupakara PV, National Symposium of Electrochemical Science and Technology Indian Science Abstracts, 43: 2006.
13. Krupakara PV, Portugaliae Electrochimica Acta, 31(3): 2013, 157-164.
14. Fontana M G, Corrosion Engineering, New York: McGraw Hill Book Company Inc., 28: 1987.
15. Sachin Govind N, Jayaprakash HV & Krupakara PV, International Journal of Innovative Research in Science, Engineering and Technology, 7: 2018, 390-394.
16. Latha V, Radha HR, Krupakara PV & Lakshmi R, International Journal of Trend in Scientific and Development (IJTSRD), International Open Access Journal, 2(4): 2018, 2810-2814.
17. Chandrashekara KN, Narasimha Murthy B, Krupakara PV & Sreenivasa K, Asian Journal of Materials Chemistry, 3(3): 2018, 47-50.
18. Jayaprakash HV, Veeraiah MK, Krupakara PV & Gireesha C, Applied Mechanics and Materials, 110: 2012, 1121-1124.
19. Radha HR, Somashekariah BV, Krupakara, PV & Vinutha K. International journal of Chemical Sciences, 7(3): 2011, 487-492.